The Astrophysical Journal, 726:113 (11pp), 2011 January 10 doi:10.1088/0004-637X/726/2/113


# TWO WIDE PLANETARY-MASS COMPANIONS TO SOLAR-TYPE STARS IN UPPER SCORPIUS

M. J. Ireland[1], A. Kraus[2,6], F. Martinache[3], N. Law[4], and L. A. Hillenbrand[5]
[1] Sydney Institute for Astronomy (SIfA), School of Physics, University of Sydney, NSW 2006, Australia
[2] Institute for Astronomy, University of Hawaii, 2680 Woodlawn Drive, Honolulu, HI 96822, USA
[3] National Astronomical Observatory of Japan, Subaru Telescope, Hilo, HI 96720, USA
[4] Dunlap Institute for Astronomy and Astrophysics, University of Toronto, 50 St. George Street, Toronto M5S 3H4, Ontario, Canada
[5] Department of Astrophysics, California Institute of Technology, MC 105-24, Pasadena, CA 91125, USA
*Received 2010 July 23; accepted 2010 November 5; published 2010 December 21*

## ABSTRACT

At wide separations, planetary-mass and brown dwarf companions to solar-type stars occupy a curious region of parameter space not obviously linked to binary star formation or solar system scale planet formation. These companions provide insight into the extreme case of companion formation (either binary or planetary), and due to their relative ease of observation when compared to close companions, they offer a useful template for our expectations of more typical planets. We present the results from an adaptive optics imaging survey for wide (∼50–500 AU) companions to solar-type stars in Upper Scorpius. We report one new discovery of a ∼14 $M_J$ companion around GSC 06214−00210and confirm that the candidate planetary-mass companion 1RXS J160929.1−210524 detected by Lafrenière et al. is in fact comoving with its primary star. In our survey, these two detections correspond to ∼4% of solar-type stars having companions in the 6–20 $M_J$ mass and ∼200–500 AU separation range. This figure is higher than would be expected if brown dwarfs and planetary-mass companions were drawn from an extrapolation of the binary mass function. Finally, we discuss implications for the formation of these objects.

*Key words:* brown dwarfs – infrared: planetary systems – planetary systems

*Online-only material:* color figures

## 1. INTRODUCTION

Over the past 5 years, direct imaging surveys for extrasolar planets have discovered a small but significant number of ultra-low mass companions (henceforth ULMCs, masses $\lesssim$20 $M_J$) at $\gtrsim$50 AU separations from their primaries. These objects have estimated masses that are in the same range as radial velocity or transiting planets with <5 AU separations, which have a continuous mass distribution up to ∼20 $M_J$, then a gap in mass until arguably star-like objects are found at >60 $M_J$ (Grether & Lineweaver 2006; Deleuil et al. 2008; Bouchy et al. 2011; Anderson et al. 2011). For this reason, ULMCs are often called "planetary-mass" companions.

The prototypical wide ULMC, 2M1207−3933, consists of a 4–8 $M_{Jup}$ companion located ∼50 AU away from a 10 Myr old brown dwarf (Chauvin et al. 2004). Since its discovery, half a dozen other ULMCs have also been reported, most of which orbit much higher-mass primaries (∼0.5–2.0 $M_\odot$; e.g., Lafrenière et al. 2008b; Kalas et al. 2008; Marois et al. 2008; Béjar et al. 2008). Some of these systems appear to be genuinely scaled-up versions of our own solar system, with planets that are consistent with formation in a disk. One example is the companion to Fomalhaut, which is coplanar with its debris disk. Another is HR 8799, which has multiple planetary companions of similar mass. Other cases like CHXR 73 and 1RXS J160929.1−210524 are more ambiguous since their orbital radii are even wider, and it is unclear whether they lie in the original plane of planet formation. Such companions could very well form like planets within a circumstellar disk or like binaries from the collapse of a molecular cloud.

These ULMCs pose a significant challenge to existing models of planet and binary formation. Their orbital radii are so large that the core accretion timescale (>100 Myr at 100 AU; Pollack et al. 1996) should be much longer than the typical protoplanetary disk dissipation timescale (∼3–5 Myr; Haisch et al. 2001; Hernández et al. 2007; Currie et al. 2009). Some of the closer companions could potentially form on the gravitational instability timescale (e.g., Boss 2001), which can be very short at intermediate radii (10–100 AU), but gravitational instability in disks has only recently been modeled at $\gtrsim$100 AU (e.g., Boley 2009; Stamatellos & Whitworth 2009). These companions could represent the extreme end of the binary mass function, which appears to be linearly flat (with all companion masses being equally probable; Kraus et al. 2008, hereafter K08; Raghavan et al. 2010) well into the substellar regime. However, it is unclear whether this trend could extend to planetary masses (by which we mean <20 $M_J$ in this paper). These companions have masses near the opacity-limited minimum mass (Hoyle 1953; Low & Lynden-Bell 1976; Bate 2005) and unless their formation occurred exactly as the circumstellar envelope was exhausted, then they should have quickly accreted enough mass to become high-mass brown dwarfs or stars.

In this paper, we report the discovery of two ULMCs in the Upper Scorpius OB association, one of which was independently discovered by Lafrenière et al. (2008b). The survey consists of a subset of the aperture-masking interferometry sample reported by K08. We describe our observations and data analysis techniques in Section 2, and in Section 2.2, we report the detections and detection limits from our survey. In Section 4, we report the first measurement of a frequency for ULMCs around young stars. Finally, in Section 5, we discuss the implications for possible formation mechanisms for ULMCs.

## 2. OBSERVATIONS

### 2.1. Discovery Observations

Nearby ($\lesssim$200 pc) young ($\lesssim$20 Myr) stars have been the object of numerous high-resolution imaging campaigns over the

[6] Hubble Fellow.

past several decades. These observations have included lunar occultation (e.g., Simon et al. 1995), speckle interferometry (e.g., Ghez et al. 1993), adaptive optics (AO) imaging (e.g., Lafrenière et al. 2007; Masciadri et al. 2005; Chauvin et al. 2010), and most recently non-redundant masking (NRM) inteferometry (K08). The earlier techniques of lunar occultation and speckle were only sensitive to the presence of bright, stellar-mass, companions, and only recently did AO imaging and NRM interferometry manage to probe within the brown dwarf regime, going as far as sampling the top of the planetary-mass regime.

In K08, we reported the results of one such survey of young stars in the Upper Sco OB association that used a combination of conventional AO imaging and NRM interferometry. In addition to the results for stellar and brown dwarf companions, that paper also reported detection limits for ULMCs at small separations (within 50 AU) where the probability of background star contamination was negligible. In this work, we report the corresponding analysis for candidate companions at wide separations, including multi-epoch follow-up imaging for three candidates, of which two appear to be associated and of approximately planetary mass.

Table 4 of K08 lists the AO imaging observations conducted with the PHARO camera at the Palomar 200″ telescope and the NIRC2 camera at the Keck II 10 m telescope. We found that 10 out of these 62 targets had stellar binary companions at separations of ∼0.″25–5.″0, which should mean that the majority of additional faint companions are not dynamically stable in this range of separation; these were omitted from our sample. In addition, we omitted the few targets with spectral types of later than M2 ($M < 0.5\,M_{\odot}$) so as to work with a single mass range of approximately "solar-type" stars, leaving 49 targets in consideration.

All observations used the smallest pixel scales (10 mas pixel$^{-1}$ with NIRC2 and 25 mas pixel$^{-1}$ with PHARO) in order to achieve the best point-spread function (PSF) sampling. We used a $K_s$ filter at Palomar and the $Br\gamma$ filter at Keck, which yielded diffraction-limited resolutions of 100 mas and 50 mas, respectively. The Keck observations used the narrowband filter despite the penalty in sensitivity, because the brighter primary stars in our sample would have saturated the detector within the minimum exposure time. Much of this sensitivity was regained by using more Fowler samples per frame, which significantly reduces the high read noise of NIRC2's detector. These observations used relatively short total integration time, of the order of a minute, in comparison with other AO imaging surveys (e.g., Metchev & Hillenbrand 2009), resulting in limiting magnitudes of $K_{\rm lim} \sim 15$–17 for the companions. Given the young age of these Upper Sco targets (∼5 Myr), even these shallow observations were able to reach the planetary-mass regime (at 2 arcsec separations, $\lesssim 14\,M_{\rm Jup}$ for 48 targets and $\lesssim 7\,M_{\rm Jup}$ for 42 targets).

The detections and detection limits were derived using methods we previously described in Kraus (2009) and A. L. Kraus & L. A. Hillenbrand (2011, in preparation). Since the detection limits at more than a few $\lambda/D$ are driven by speckle noise, detections and detection limits were determined from the co-added image stacks by placing a large number of photometric apertures (with diameter $\lambda/D$) around each target, then measuring the mean and standard deviation of the brightness distribution for all apertures in concentric rings around the primary. For each ring, we identified all candidate detections with significance $\gtrsim 5\sigma$ above the mean brightness, then compared those detections to other stars taken on the same night to identify and reject the quasi-static speckles and diffraction spikes that are seen in common for many targets. All candidate detections that could not be identified as PSF artifacts were then adopted as genuine sources and hence as candidate bound companions, while the $5\sigma$ limits were adopted as our formal detection limits. At large separations, the detection limit from this algorithm converges to the sky background limit, and at these separation (>2 arcsec), we used a $10\sigma$ limit, because of the large number of pixels in this regime. We found no candidate companions near the detection limits in the speckle-limited regime, but there are many candidate companions in the sky-limited regime.

We determined the photometry and astrometry for these sources using the methods described in K08 and Kraus & Hillenbrand (2009). To briefly summarize, we measured astrometry and aperture photometry for each source with respect to the known USco member using the IRAF task DAOPHOT (Stetson 1987); all measurements were conducted using apertures of 0.5, 1.0, and 2.0 $\lambda/D$, and then the optimal aperture was chosen to maximize the significance of the detection (given the competing uncertainties from the sky background and the Poisson noise for the source itself). In order to estimate the uncertainties from the data, we analyzed the measurements in individual frames and then combined those measurements to estimate the mean and standard deviation. We then accounted for the systematic uncertainty in the plate scales and distortion solutions of PHARO (0.3%; Section 2.2) and NIRC2 (0.05%; Ghez et al. 2008; Cameron 2008) by adding those terms in quadrature with the observed scatter. Most of the new candidate companions were identified with PHARO; as we describe below, its astrometric calibration is not yet well understood and might be further improved with more calibration observations, but our systematic uncertainties should account for this effect. Many of the wider ($\gtrsim 5''$) companions are also affected by anisoplanatism, yielding systematically low brightness estimates for aperture photometry. A correction of the photometry would require a detailed knowledge of the atmospheric turbulence profile and isoplanatic patch size, so it cannot be accomplished for our data. However, as we describe below, all of these sources have well-calibrated $K$ magnitudes available from UKIDSS. We choose instead to defer to those measurements in determining colors (Section 3.2).

Finally, all candidate companions with separations $\gtrsim 4.''2$ have spatially resolved counterparts in the UKIDSS Galactic Cluster Survey (Lawrence et al. 2007), and many of the widest companions also have optical counterparts in the USNO-B1.0 digitization of the Palomar Observatory Sky Survey (Monet et al. 2003). As we describe further in Section 3.2, we have used those observations to identify most of these candidate companions as background stars. The rest require multi-epoch astrometric monitoring to determine whether they are associated.

### 2.2. Follow-up Observations

Around three targets in the K08 survey we found faint visual candidate companions with projected separations of 2″–3″ and brightnesses of $K \sim 15$–16: GSC 06214−00210, 1RXS J160929.1−210524, and 1RXS J160703.4−203634, whose basic properties are listed in Table 1. In this section we will describe the requirements for follow-up observations of these targets, and why the NIRC2 camera was chosen for follow-up rather than PHARO. The follow-up observations including the filters used are detailed in Table 2.

The expected surface density of unassociated background stars at these brightnesses is relatively low, but since Upper Scorpius is at moderate galactic latitude and is projected over

**Table 1**
Stellar Properties

| Name | R.A. (J2000) | Decl. (J2000) | SpT | Mass ($M_\odot$) | $R$ (mag) | $K$ (mag) |
|---|---|---|---|---|---|---|
| GSC 06214−00210 | 16 21 54.67 | −20 43 09.1 | M1 | 0.60 | 11.6 | 9.15 |
| 1RXS J160929.1−210524 | 16 09 30.30 | −21 04 58.9 | K7/M0 | 0.68−0.77 | 12.1 | 8.92 |
| 1RXS J160703.4−203634 | 16 07 03.56 | −20 36 26.5 | M0+? | 0.68+0.59 | 11.3 | 8.10 |

**Notes.** $R$ magnitudes are from USNO-B, while coordinates and $K$ magnitudes are from 2MASS. The mass of the secondary star for 1RXS J160703.4−203634 is inferred from the mass ratio, while other masses are directly inferred from the mass–temperature relations of Baraffe et al. (1998). Spectral types are taken from the discovery sources, Preibisch et al. (1998) and Kunkel (1999).

**Table 2**
Follow-up Observations

| Julian Date | Band | Separation (mas) | Position Angle (deg) | Contrast (mag) |
|---|---|---|---|---|
| GSC 06214−00210 b | | | | |
| 2454258.0 | $K_p$ | 2203.3 ± 1.5 | 176.04 ± 0.06 | 5.74 ± 0.05 |
| 2454634.8 | $K_p$ | 2204.7 ± 0.9 | 175.99 ± 0.03 | 5.78 ± 0.03 |
| 2454634.8 | $J$ | 2205.2 ± 0.9 | 176.00 ± 0.09 | 6.30 ± 0.03 |
| 2454982.9 | $K_p$ | 2204.1 ± 0.9 | 175.91 ± 0.03 | 5.88 ± 0.03 |
| 2455313.1 | $K_p$ | 2205.6 ± 1.1 | 175.93 ± 0.03 | 5.73 ± 0.03 |
| 2455313.1 | $H$ | 2202.8 ± 2.2 | 175.91 ± 0.04 | 6.21 ± 0.03 |
| 2455313.1 | $L'$ | ... [a] | ... [a] | 4.75 ± 0.05 |
| 1RXS J160929.1−210524 b | | | | |
| 2454634.8 | $K_p$ | 2210.1 ± 1.0 | 27.62 ± 0.04 | 7.27 ± 0.02 |
| 2454982.9 | $K_p$ | 2211.3 ± 0.9 | 27.61 ± 0.05 | 7.23 ± 0.03 |
| 1RXS J160929.1−210524 c | | | | |
| 2454250.8 | $K_s$ | 4261 ± 14 | 219.5 ± 0.2 | 8.63 ± 0.04 |
| 2454982.9 | $K_p$ | 4215 ± 5 | 220.03 ± 0.08 | 8.6 ± 0.1 |
| 1RXS J160703.4−203634 b | | | | |
| 2454634.8 | $K_p$ | 2143.2 ± 1.5 | 234.01 ± 0.07 | 8.20 ± 0.08 |
| 2454634.8 | $J$ | 2138.2 ± 1.0 | 234.05 ± 0.07 | 8.06 ± 0.05 |
| 2454982.9 | $K_p$ | 2123.1 ± 0.5 | 234.45 ± 0.01 | ... [b] |

**Notes.**
[a] Data not suitable for precision astrometry.
[b] Data were taken through the `corona400` coronagraph at 1.04 ± 0.03 mag contrast and ∼7 mag extinction of the primary (not precisely calibrated).

the background Milky Way bulge, this probability was not sufficiently low so that we could assume they were bound ULMC companions. Follow-up observations were therefore required to confirm common proper motion.

The density of background stars at $K < 17$ is approximately 0.002 arcsec$^{-2}$ (A. L. Kraus & L. A. Hillenbrand 2011, in preparation), which gives an 86% chance of a chance alignment within 2.″5 for at least one star in our sample, but only a 30% chance of all three candidates being chance alignments. It is impossible to use proper motions to rule out chance alignments with other association members because the internal velocity dispersion of Upper Sco is only ∼1 km s$^{-1}$ (∼1.5 mas yr$^{-1}$; Kraus & Hillenbrand 2008), meaning that they would be comoving even if they were only seen in chance alignment. However, the surface density of young stars in Upper Sco is no more than 100 deg$^{-2}$ (Kraus & Hillenbrand 2008) or $10^{-5}$ arcsec$^{-2}$, meaning that the probability of a chance alignment is negligible.

The proper motion of the Upper Scorpius association is (−11.5, −23.5) mas yr$^{-1}$ in equatorial coordinates, determined from the members listed in de Zeeuw et al. (1999), and using updated proper motions from van Leeuwen (2007). This is relatively small when compared to nearby moving groups, so an astrometric accuracy of order 2 mas or 0.1% at 2″ is required in order to clearly determine whether a companion is comoving or not on a 1 year time baseline.

The NIRC2 camera has been shown to have a stability better than this in the precise galactic center astrometric work of Ghez et al. (2008). Cameron et al. (2009) showed that the PALMAO AO system (Troy et al. 2000) and the PHARO near-infrared (NIR) camera are stable in distortion to ∼100 $\mu$as over several months. However, PALMAO underwent several upgrades between these common proper motion confirmation observations, including preliminary work for a reconfiguration of the output beam path to accommodate new science instruments.

We searched for PALMAO distortion solution changes during this period using observations of the core of the M5 globular cluster from four nights (2007 May 28, 2007 May 29, 2008 July 17, and 2008 August 17). The observations consisted of 100 co-added 1.4 s exposures at each epoch were taken in the 25 mas PHARO plate scale, used the $Br\gamma$ narrowband filter to avoid differential chromatic refraction, and were timed to be observed at very similar airmasses and hour angles. The same AO guide star was used in each case, and care was taken to align each epoch to the same pointing within an arcsecond and to keep all other AO and camera parameters consistent. We fitted two-dimensional Gaussians to derive the positions of 34 stars covering the 25″×25″ field in each data set; we also checked

the fitted positions using SExtractor (Bertin & Arnouts 1996) and found very similar results.

We first used a simple model to match the stellar positions between epochs, allowing for a change in pointing position, an arbitrary rotation, and a separate scaling in the *X*- and *Y*-axes. There was no detectable change in rotation or scale within 2007 or within 2008, but between those years the field rotation changed by 0.18 deg, while the *X* and *Y* plate scales changed by −0.5% and +0.2%, respectively. However, the simple rotation and plate scale change model leaves 3–5 mas residuals in matching the 2007 and 2008 measured positions. The residuals are reduced to ∼1 mas using a general four-parameter linear transformation, where the additional parameter represents the plate scale changes being in arbitrary orthogonal axes, or alternatively the addition of a shear term. However, some statistically significant higher-order distortion is still apparent after application of this solution. It appears that long-term precision astrometry using AO requires careful attention to changes in the detailed distortion solutions (beyond simple rotation and scale); this is particularly important as, like PALMAO, the optics of many AO systems are regularly upgraded.

Therefore, wherever at least two NIRC2 epochs are available, we only consider the astrometry with NIRC2 for our proper motion measurements. All follow-up NIRC2 data were acquired using the narrow camera with a ∼10 mas pixel$^{-1}$ image scale and the $K_p$ filter, which we found did not quite saturate for these targets using the shortest exposure time with a minimum number of Fowler samples.

The follow-up NIRC2 data were reduced using a custom pipeline written in IDL. After standard image-processing tasks (background subtraction, flat-fielding, and bad pixel removal) were completed, the distortion in the image plane was then removed by the program `nirc2dewarp` available from the NIRC2 camera home page, using the updated distortion solution of B. Cameron (2007, private communication). Finally, aperture photometry and centroids were computed with the `ImExam` function of `atv`, version 2.0b4. Selected data sets were also analyzed with the DAOPHOT function of IRAF, giving results consistent well within the error bars.

For centroiding, a centering box size of 5 pixels was used, with the exception of one single observation in *L* band, where a box size of 9 pixels was used. The aperture radius for photometry was 5 pixels for the $K_p$ filter, but 7 pixels for the *J* and *H* filters due to low Strehls and dispersion, and 10 pixels in *L* band due to the larger diffraction-limited core. The sky annulus was always set at 10–20 pixels. Note that we did not attempt to calibrate absolute photometry and have only computed the relative photometry between primary and secondary.

## 3. RESULTS

The following subsections describe the multi-epoch astrometry obtained on each of the three targets in Table 1, in order to confirm proper motion. Two clearly associated objects are discussed as well as two objects identified as background stars.

### 3.1. New Companions

#### 3.1.1. GSC 06214−00210 b

GSC 06214−00210 is a young M1 star near the eastern edge of Upper Sco. It was originally identified as a candidate young star by Preibisch et al. (1998) based on its X-ray emission, then confirmed to have strong lithium absorption (EW = 0.38 Å) and H$\alpha$ emission (EW = −1.51 Å) as compared to stars of

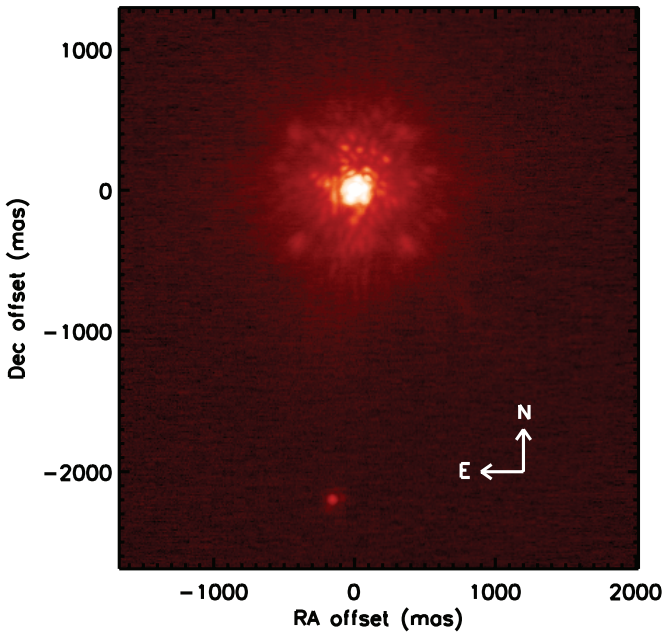


**Figure 1.** Example image of GSC 06214−00210 from 2008 July in the $K_p$ filter, with a log stretch. The faint companion can be seen as at an R.A. offset of ∼ −200 mas and a decl. offset of ∼ −2200 mas.

(A color version of this figure is available in the online journal.)

equivalent spectral type in several young clusters. It was also found to have a proper motion $\mu = (-18.6 \pm 1.7, -32.2 \pm 1.7)$ mas yr$^{-1}$ (Zacharias et al. 2010), consistent with the motion of Upper Sco. Given its M1 spectral type, the 5 Myr mass–temperature relations of Baraffe et al. (1998) predict a mass of 0.60 $M_\odot$. Note that this mass must be taken with caution, as an uncertainty of 1 subclass in spectral type should correspond to an uncertainty of ∼0.1 $M_\odot$ in mass. One should keep in mind that the models themselves carry an unknown uncertainty since the mass–luminosity and mass–temperature relations of young stars are almost completely uncalibrated for $\lesssim$1 $M_\odot$ (e.g., Hillenbrand & White 2004).

An example image of GSC 06214−00210b used for astrometry is shown in Figure 1. Our photometric and astrometric observations of this companion are given in Table 2 and Figure 2. The candidate companion showed a relative motion of 7 ± 4 mas with respect to GSC 06214−00210 over 2.9 years. This is much less than the ∼70 mas motion expected if GSC 06214−00210b were a background star and demonstrates that it is most likely physically associated with GSC 06214−00210. The apparent relative proper motion of 2.5±1.3 mas yr$^{-1}$ corresponds to 1.7 ± 0.9 km s$^{-1}$ assuming a 7 mas parallax for Upper Scorpius, which is roughly equal to the circular orbital velocity of 1.7 km s$^{-1}$ expected for a ∼300 AU orbit.

As can be seen from the larger contrast in bluer filters (cf. Table 2), GSC 06214−00210b is quite red compared to its primary star. The primary has an observed Two Micron All Sky Survey (2MASS) color of $J - K = 0.85 \pm 0.04$, and most M1 stars have a typical $K - L'$ color of ∼0.15 ± 0.05 (Leggett 1992), so the inferred colors for the companion are $J - K = 1.35 \pm 0.11$ and $K - L = 1.18 \pm 0.10$. The mean distance for Upper Sco is 145 pc (de Zeeuw et al. 1999), and a ±6 deg spread on the sky of the densest region (where all our candidates belong) corresponds to a ∼14 pc error on the distance of any individual star. This gives a distance modulus of $m - M = 5.8 \pm 0.2$,

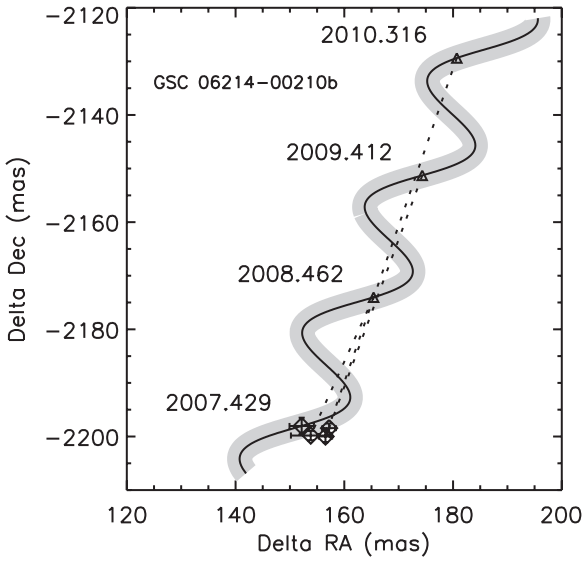


**Figure 2.** Observed position of the companion to GSC 06214−00210 (diamonds), with the expected motion of the companion if it were a background star with respect to the first epoch overplotted (solid line, triangles at the times of observation). The dashed lines join the locations of the companion at each epoch with the expected position if it were a background star. This shows that GSC 06214−00210b is physically associated.

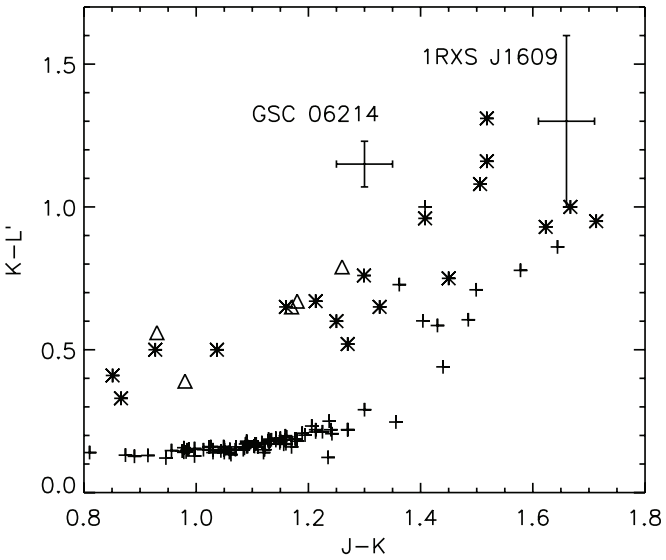


**Figure 3.** $J - K$ vs. $K - L'$ color for our two confirmed companions, with the colors overplotted for M dwarfs from Leggett (1992) (triangles), M4 to L6 dwarfs from Golimowski et al. (2004) (asterisks), and for M giants from Fluks et al. (1994) (crosses). The $L$-band photometry of 1RXS J160929.1−210524 comes from Lafrenière et al. (2010).

so given the 2MASS magnitudes of the primary, the absolute magnitudes of the companion are $M_J \sim 10.5$, $M_H \sim 9.6$, $M_K \sim 9.1$, and $M_{L'} \sim 7.9$. The interstellar extinction toward Upper Sco is negligible ($A_V \lesssim 1$ or $A_K \lesssim 0.1$), so no extinction corrections should be required.

The observed $J - K$ color of 1.3 is consistent with the M8–L4 spectral type range of field dwarfs from Leggett et al. (2002). The $K - L$ color of 1.05, however, would clearly place the star at the red end of this range, at L3–L4. The absolute $K$ magnitude of 9.1 is then about 2 mag brighter than for corresponding field objects, providing clear evidence of a larger radius and young age; this height above the main sequence is similar to that observed for other late-type members of Upper Sco (Lodieu et al. 2007) and TW Hya (Mamajek 2005; Teixeira et al. 2008).

The colors and spectral type of GSC 06214−00210b are not expected to match field dwarfs due to the low surface gravity. Allers et al. (2010) find that $J - K$ and $K - L$ colors are significantly redder for low gravity objects at a given spectral type. Although GSC 06214−00210b is a low-mass object, Allers et al. (2010) focus on redder objects at $J - K$ colors of ∼2.0, and it is not clear that their result should hold for bluer objects like GSC 06214−00210b, with $J - K = 1.3$. In Figure 3, we show the NIR, the colors of GSC 06214−00210b with respect to field dwarfs and giants (which bracket GSC 06214−00210b in gravity), where it appears to have a small but significant $K - L'$ excess. The red $K - L$ color could be due to a disk, as $\gtrsim$1/3 of young brown dwarfs retain a disk for $\gtrsim$5 Myr (e.g., Scholz et al. 2007), with a trend of increasing disk lifetime with decreasing mass. Spatially resolved spectroscopy of the system would be required in order to determine the spectral type more accurately, and to search for signs of accretion onto the secondary.

Given the observed brightness in the *JHK* filters, a comparison to the 5 Myr DUSTY models (Chabrier et al. 2000) et al. 2000) suggests that the mass of the companion is ∼12–15 $M_{\rm Jup}$, with bluer filters suggesting slightly lower masses than redder filters. The COND models (Baraffe et al. 2003) never predict sufficiently red $J - K$ colors to match our observations, and indeed are not appropriate for objects with $T > 1300$ K. This trend qualitatively matches the observed trend for young low-mass objects to be redder than older field counterparts of similar spectral type. If the comparison was based only on observed $J - K$ color, then the DUSTY models would predict masses of 10–12 $M_{\rm Jup}$. As we discussed above, the $L'$ photometry could have an excess from a circumstellar disk, so we suggest that the $L'$ magnitude should not be used directly in the mass estimate.

#### *3.1.2. 1RXS J160929.1−210524 b*

1RXS J160929.1−210524 is a young M0 star located near the center of Upper Sco. Like GSC 06214−00210, it was first identified as a likely Upper Sco member by Preibisch et al. (1998) and exhibits both strong lithium absorption (EW = 0.54 Å) and H$\alpha$ emission (EW = −1.14 Å). The proper motion reported by UCAC3 (Zacharias et al. 2010) for this object is (−11.2, −21.9) ±1.5 mas yr$^{-1}$, which is also consistent with the value for Upper Sco. The spectral type reported by Preibisch et al. (1998) was M0, but, as was described by Lafrenière et al. (2008b), newer measurements by D. C. Nguyen suggest a more likely spectral type of K7. The inferred mass would be 0.68–0.77 $M_\odot$ for the two estimates, with uncertainties similar to that for GSC 06214−00210.

Our observations for 1RXS J160929.1−210524 b are listed in Table 2 and plotted in Figure 4. The companion was first detected in Palomar images as early as 2007 May, but as the astrometric performance of the PHARO camera was unverified on large timescales (cf. Section 2.2), we were not able to convincingly demonstrate common proper motion until 2009. This object was independently detected by Lafrenière et al. (2008b) and further characterized by Lafrenière et al. (2010). Our astrometric results are consistent with those recently reported by Lafrenière et al. (2010) at 2$\sigma$ in separation and at 1$\sigma$ in position angle, but have higher precision due to the accurate astrometric characterization of NIRC2. Based on a spectrum indicating a late spectral type and low gravity, these authors argued that this faint companion was a young object and therefore likely a physical companion.

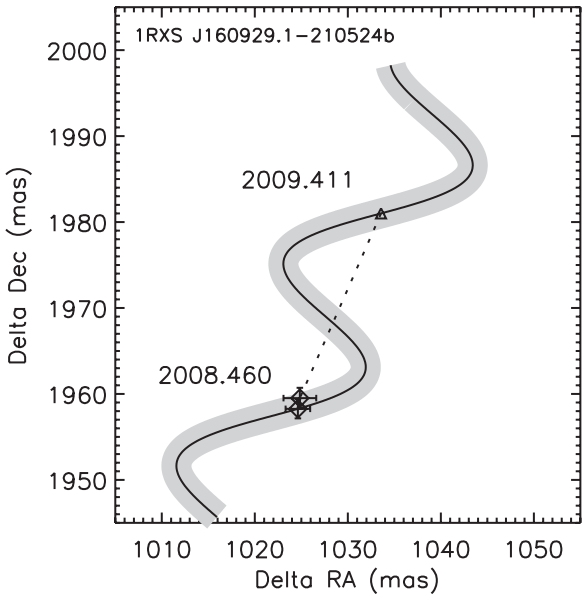


**Figure 4.** Observed position of the closer companion to 1RXS J160929.1−210524, with symbols as in Figure 2. The two observations are at nearly indistinguishable locations in this plot, demonstrating that the companion is physically associated.

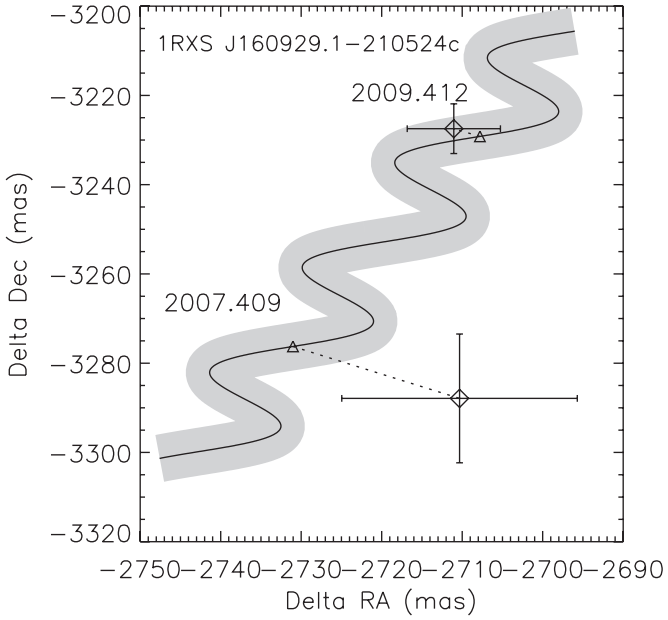


**Figure 5.** Observed position of the wider companion to 1RXS J160929.1−210524, with symbols as in Figure 2. As the first epoch has such large errors, we reference the apparent motion expected from a background star to the weighted average of the two epochs rather than to the first epoch. Motion of 1RXS J160929.1−210524 with respect to this object is clearly detected, demonstrating that the candidate companion is a background star.

Since that time, we have continued monitoring this object (cf. Table 2) and can now confirm that 1RXS J160929.1−210524 b is a physical companion of 1RXS J160929.1−210524. The apparent proper motion of $1.2 \pm 1.3$ mas yr$^{-1}$ corresponds to $0.8 \pm 0.9$ km s$^{-1}$. This is consistent with the $\sim$1.7 km s$^{-1}$ orbital motion expected, especially considering possible projection effects.

Since Lafrenière et al. (2008b) already reported NIR colors, we only took $K$-band observations. These measurements are consistent with theirs and indicate an absolute magnitude of $M_K \sim 10.4$. The predicted mass from the DUSTY and COND models is $\sim 8\,M_{\rm Jup}$ from the $K$-band photometry or $\sim 7\,M_{\rm Jup}$ from $J$-band photometry, though again, these estimates are completely uncalibrated by observations. Given the assumptions listed above for the distance of Upper Sco, the projected separation is $\sim$320 AU, similar to the value for GSC 06214−00210 system.

### 3.2. Background Stars

Unassociated background stars typically are identified based on multi-epoch astrometric monitoring (which indicates that they are not comoving) or multi-wavelength observations to measure colors (which indicate that they do not fall along the same color–magnitude sequence). As we describe in the next several subsections, several of the closer companions will require astrometric monitoring with high-resolution imaging to confirm or disprove their association, but the wider companions can be identified and rejected based on archival photometry from seeing-limited all-sky surveys.

#### 3.2.1. 1RXS J160929.1−210524 c

In addition to the companion listed as companion b in Table 2, an additional wider companion candidate, listed as companion c in Table 2 was found around 1RXS J160929.1−210524 in both the 2007 Palomar images (see Section 3.2.3) and the 2009 Keck images. This companion candidate was also reported by Lafrenière et al. (2008b). Although the Palomar astrometry had significant errors, the time baseline of 2 years was sufficient to clearly show that this object was a background star, as shown in Figure 5.

#### 3.2.2. 1RXS J160703.4−203634 b

1RXS J160703.4−203634 is a young, close binary system which is also located near the center of Upper Sco. It was originally identified in a survey for new Sco-Cen members by Kunkel (1999), using methods very similar to the survey by Preibisch et al. (1998): targets were identified as potential X-ray emitters, then confirmed to have strong lithium for their age. However, the survey by Kunkel was never published in the refereed literature, so the equivalent widths of relevant spectral lines are not available. We discovered its multiplicity during our direct imaging and aperture-masking survey (K08), finding that it had a companion with projected separation of 184 mas ($\sim$27 AU) and flux ratio $\Delta K = 0.15$ (mass ratio $q \sim 0.87$). The same observations also revealed a faint candidate companion at a projected separation of $\sim 2\farcs1$.

As we summarize in Table 2 and Figure 6, multi-epoch astrometry for the candidate companion shows that it is not comoving with 1RXS J160703.4−203634, but instead appears to be nearly stationary, as would be expected for a background star. The relative motion of the primary with respect to the companion is $(7 \pm 2, -26 \pm 2)$ mas yr$^{-1}$, consistent with the proper motion of Upper Scorpius.

The contrast with respect to the brighter member of the close binary pair is $\Delta K = 8.15 \pm 0.08$ and $\Delta J = 8.06 \pm 0.05$, indicating that the companion has a color of $J - K = 0.90 \pm 0.10$. Given that the total extinction along this line of sight is only $A_V \sim 1.2$ or $E(J-K) \sim 0.2$ (Schlegel et al. 1998), the companion must be intrinsically cool ($J - K \gtrsim 0.7$ or spectral type $\gtrsim$K5; Kraus & Hillenbrand 2007). Combined with its non-motion (which indicates that it is likely to be quite distant),

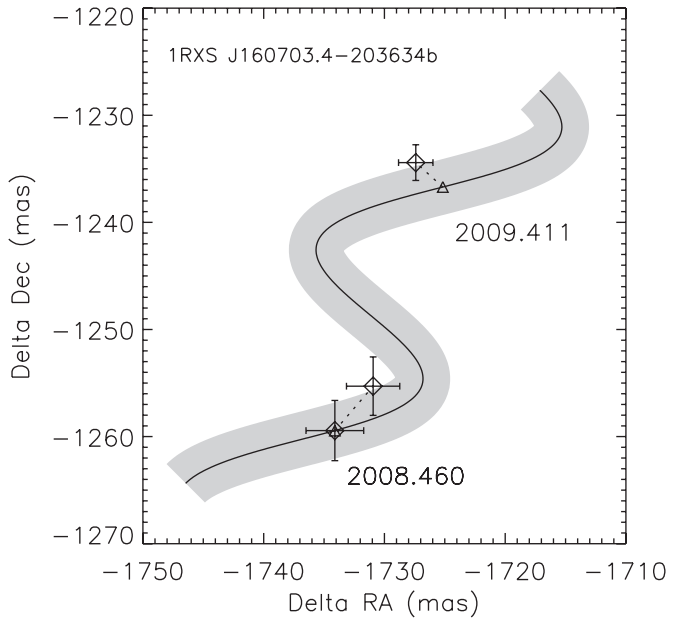


**Figure 6.** Observed position of the companion to 1RXS J160703.4−203634 with respect to the center of light of the close binary, with symbols as in Figure 2. This candidate companion is consistent with a background star.

we therefore conclude that the candidate companion is likely a background K or early M giant, perhaps located in the Milky Way bulge.

#### 3.2.3. Wider Potential Companions

Multi-epoch observing campaigns can be observationally expensive, so where possible, it is best to use archival data to rule out possible companions. This is sometimes impossible since many candidate companions of interest can only be distinguished from their candidate primary using high-resolution imaging techniques. However, wider companions can often be resolved in seeing-limited data, especially for new surveys that have very good spatial resolution (i.e., $\lesssim$0.″5 for UKIDSS images).

Of the 25 companions with separations of $\gtrsim$3.″5, 21 were detected in both the $H$ and $K$ filters by UKIDSS (DR7), so we can use their $H - K$ colors to determine whether they might be associated. UKIDSS observations of known low-mass members of Upper Sco by Lodieu et al. (2007) show that most members fainter than $K \sim 13$ (i.e., with spectral type $\gtrsim$M7) have colors of $H - K > 0.5$; this limit is consistent with the typical $H - K$ colors of $\gtrsim$M7 field dwarfs as compiled in Kraus & Hillenbrand (2007). As we show in Table 3, none of the candidate companions with both $H$ and $K$ magnitudes meet this criterion, so we identify all of them to be unassociated field stars, most likely in the distant background behind Upper Sco.

In addition, 17 of the wider candidate companions have counterparts visible in the USNO-B1.0 digitization of the Palomar Observatory Sky Survey (Monet et al. 2003). Most are not present in the USNO-B1.0 source catalog since its source identification algorithm was extremely conservative in identifying faint neighbors to bright stars. However, these sources can be manually identified by visual inspection. In Table 3, we list the bluest plate ($B$ or $R$) at which each of the companions was visible. As we noted above, any true companions should have spectral types of $\gtrsim$M7, so our compilation of field dwarf colors (Kraus & Hillenbrand 2007; A. L. Kraus & L. A. Hillenbrand 2011, in preparation) suggests that the expected colors for true companions are $B - K > 9$ and $R - K > 6$. The detection limits of the POSS survey were $B \sim 21$ and $R \sim 20$, so all 17 sources with counterparts in the $B$ or $R$ plates must be background stars that are bluer than these limits. In all cases, these identifications agree with the UKIDSS identification.

Three wider companions in Table 3 cannot be eliminated as Upper Scorpius members due to insufficient photometry or astrometry. These are the companions to GSC 06793−00994, GSC 06794−00156, and ScoPMS 015. The closest of these systems is ScoPMS 015, with a companion just outside of 500 AU. This small incompleteness defines the outer limit of our survey until additional follow-up observations can be obtained, though some azimuthal uncertainty remains at separations of <500 AU due to image boundaries (Section 3.3).

### 3.3. Detection Limits

In order to infer the properties of the distribution of wide ULMCs, it is essential not only to establish the existence of a small number of physical companions, but also to determine the magnitude limit as a function of separation for possible companions not confidently identified in the observations. This has not been general practice in previously reported wide ULMCs, in particular not for several of the $\lesssim$40 $M_J$ companions in our separation and primary mass range: GQ Lup b, CT Cha b, and 1RXS J160929.1−210524 b. In this section, we will describe the detection limits for all stars in our sample.

As we described in Section 2.1, we measured our detection limits in a method that accounts for both spurious detections from speckle noise (at small separations) and the sky background limit (at large separations). These limits could in principle be used as input for Monte Carlo or Bayesian techniques to study the underlying population, though as we discuss in Section 4, using the results from our survey alone could yield a biased measurement.

Table 4 lists and Figure 7 shows the companion detection limits for each star in the sample. The last column of Table 4 also gives the maximum separation in arcseconds where we surveyed all position angles for companions. The few small ($\lesssim$3″) values of $\rho_{100\%}$ in this column are due to quick image sets taken in the camera sub-array mode we used for aperture-masking interferometry. The limits at separations smaller than 1″ are set by the separation-dependent speckle noise and extended PSF halo of the primary star, while the wider limits at separation greater than 1.″5 are constant and result from the sky background (for broadband $K$ observations) or read noise (for narrowband $Br\gamma$ observations). For each star, we list the primary $K$ magnitude (from 2MASS, with the flux from any close binary companions subtracted), the detection limit in $K_{sec}$ at a range of angular separation, and the corresponding detection limit in $M_{Jup}$ at the corresponding projected orbital distances. The mass detection limits were derived from the $K$ magnitudes of the 5 Myr DUSTY isochrone (Chabrier et al. 2000).

## 4. THE FREQUENCY OF WIDE ULTRA-LOW MASS COMPANIONS

The most basic step in assessing the ability of current planet formation theories (see Section 1) to explain the widely separated and relatively massive candidate planetary companions

**Table 3**
Faint Candidate Companions to Young Stars in Upper Scorpius

| Known Member | $\rho$ (mas) | P.A. (deg) | $\Delta K$ (mag) | USNO-B1.0 (color/epoch) | $H_{\rm UKIDSS}$ (mag) | $K_{\rm UKIDSS}$ (mag) | $H-K$ (mag) |
|---|---|---|---|---|---|---|---|
| RXJ1603.6−2245 | 10959 ± 34 | 206 ± 0.2 | 7.52 ± 0.03 | R2 | 15.339 ± 0.011 | 15.074 ± 0.013 | 0.265 ± 0.017 |
| RXJ1603.9−2031A | 9484 ± 29 | 280 ± 0.2 | 7.49 ± 0.04 | B2 | 15.668 ± 0.012 | 15.547 ± 0.018 | 0.121 ± 0.022 |
| RXJ1606.2−2036 | 6820 ± 22 | 62.6 ± 0.2 | 7.07 ± 0.07 | ... | 16.449 ± 0.022 | 16.306 ± 0.034 | 0.143 ± 0.040 |
| RXJ1607.0−2036 | 11939 ± 36 | 47.7 ± 0.2 | 6.50 ± 0.03 | B2 | 15.573 ± 0.010 | 15.433 ± 0.015 | 0.140 ± 0.018 |
| USco-160517.9−202420 | 7638 ± 4 | 153.998 ± 0.013 | 6.23 ± 0.02 | B2 | 15.299 ± 0.009 | 15.173 ± 0.013 | 0.126 ± 0.016 |
| USco-160801.4−202741 | 7175 ± 24 | 323.8 ± 0.2 | 6.88 ± 0.11 | ... | 16.344 ± 0.029 | 16.145 ± 0.039 | 0.199 ± 0.049 |
| USco-160801.4−202741 | 10666 ± 32 | 69.1 ± 0.2 | 6.67 ± 0.04 | B2 | 16.053 ± 0.022 | 15.959 ± 0.033 | 0.094 ± 0.040 |
| USco-160900.7−190852 | 6850 ± 27 | 274.2 ± 0.2 | 7.06 ± 0.05 | B2 | 15.571 ± 0.012 | 15.406 ± 0.017 | 0.165 ± 0.021 |
| GSC 06205−00954 | 15398 ± 47 | 183.7 ± 0.2 | 5.03 ± 0.02 | B2 | 13.887 ± 0.003 | 13.723 ± 0.004 | 0.164 ± 0.005 |
| GSC 06209−01501 | 8994 ± 27 | 216.6 ± 0.2 | 8.17 ± 0.04 | B2 | 16.513 ± 0.033 | 16.51 ± 0.055 | 0.003 ± 0.064 |
| GSC 06213−01358[a] | 4261 ± 14 | 219.5 ± 0.2 | 8.63 ± 0.04 | ... | ... | ... | ... |
| GSC 06793−00797 | 11086 ± 33 | 116.4 ± 0.2 | 6.46 ± 0.02 | B2 | 14.426 ± 0.005 | 14.339 ± 0.008 | 0.087 ± 0.009 |
| GSC 06793−00797 | 12330 ± 38 | 223.3 ± 0.2 | 4.46 ± 0.03 | B2 | 12.265 ± 0.001 | 12.121 ± 0.001 | 0.144 ± 0.001 |
| GSC 06793−00994 | 5462 ± 17 | 357.4 ± 0.2 | 7.79 ± 0.04 | ... | ... | 15.400 ± 0.018 | ... |
| GSC 06794−00480 | 11820 ± 36 | 313.0 ± 0.2 | 6.41 ± 0.03 | B2 | 15.072 ± 0.008 | 14.726 ± 0.010 | 0.346 ± 0.013 |
| GSC 06214−00210 | 12941 ± 39 | 30.4 ± 0.2 | 5.88 ± 0.02 | B2 | 14.507 ± 0.006 | 14.415 ± 0.008 | 0.092 ± 0.010 |
| GSC 06794−00537 | 15942 ± 49 | 81.5 ± 0.2 | 8.29 ± 0.06 | ... | 16.310 ± 0.023 | 15.951 ± 0.030 | 0.359 ± 0.038 |
| GSC 06794−00537 | 5214 ± 16 | 73.6 ± 0.2 | 7.99 ± 0.04 | ... | 15.548 ± 0.012 | 15.433 ± 0.019 | 0.115 ± 0.022 |
| GSC 06794−00156 | 5973 ± 18 | 338.7 ± 0.2 | 9.43 ± 0.04 | ... | ... | 15.029 ± 0.013 | ... |
| ScoPMS 015 | 16954 ± 51 | 180.8 ± 0.2 | 8.02 ± 0.07 | B2 | 16.664 ± 0.033 | 16.491 ± 0.044 | 0.173 ± 0.055 |
| ScoPMS 015 | 3538 ± 11 | 94.9 ± 0.2 | 7.19 ± 0.02 | ... | ... | ... | ... |
| ScoPMS 015 | 7485 ± 23 | 25.7 ± 0.2 | 7.20 ± 0.03 | B2 | 16.085 ± 0.020 | 16.054 ± 0.030 | 0.031 ± 0.036 |
| ScoPMS 015 | 12482 ± 38 | 47.0 ± 0.2 | 7.06 ± 0.04 | B2 | 16.773 ± 0.036 | 16.618 ± 0.049 | 0.155 ± 0.061 |
| ScoPMS 045 | 7063 ± 21 | 190.3 ± 0.2 | 8.44 ± 0.04 | B2 | 16.408 ± 0.029 | 16.134 ± 0.029 | 0.274 ± 0.041 |
| ScoPMS 045 | 11286 ± 34 | 173.5 ± 0.2 | 7.76 ± 0.03 | B2 | 16.216 ± 0.024 | 15.970 ± 0.025 | 0.246 ± 0.035 |

**Note.** [a] See Section 3.1.2 for multi-epoch astrometry of this object.

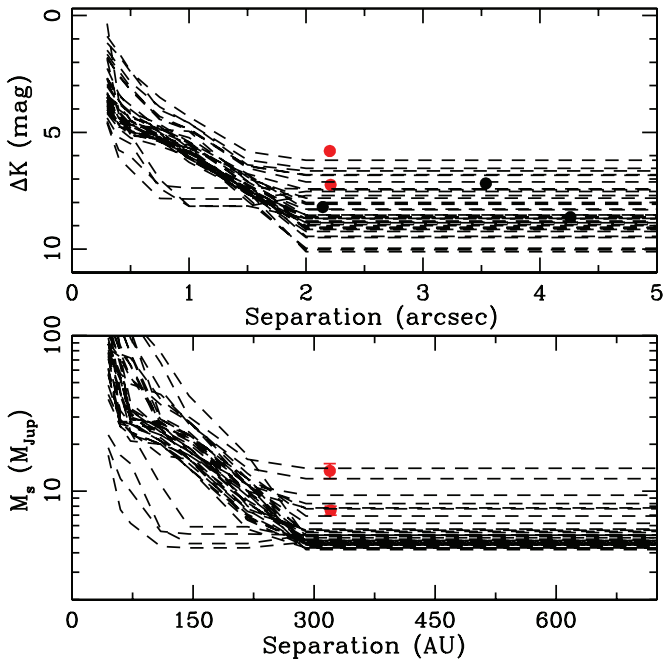


**Figure 7.** Detections and detection limits for our direct imaging observations of young stars in Upper Sco. Top: contrast limits ($\Delta K$ in mag) as a function of angular separation (in arcseconds). Bottom: corresponding limits in terms of secondary mass (in $M_{\rm Jup}$) and physical separation (in AU). The detection limits are shown with black dashed lines, the two confirmed ULMCs are shown with red points, and all other candidate companions (most of which are confirmed as background stars) are shown with black points. We have truncated the plot at a maximum separation of 5″ since deep seeing-limited imaging from UKIDSS demonstrates that all wider companions are unassociated field stars (Section 3.2.2).

(A color version of this figure is available in the online journal.)

that are observed is to measure their frequency. Most of the 49 stars in our sample have relatively uniform detection limits (∼4–6 $M_{\rm Jup}$ at $\gtrsim$300 AU), so a naive estimate of the frequency is approximately $2/49 = 4.1^{+4.9}_{-1.3}$%. Here, we have quoted the most likely frequency and the Bayesian 68% confidence interval on the frequency with a prior distribution where all frequencies are equally likely. The detection limits are not completely uniform, so the exact frequency will depend on more sophisticated analysis using Monte Carlo (K08) or Bayesian (Allen 2007; A. L. Kraus and L. A. Hillenbrand 2011, in preparation) techniques, and ultimately should depend on the separation and mass distributions of ULMCs.

There is also a more fundamental issue that must be considered: this survey is not the first to be sensitive to the presence of ULMCs, and a full treatment should consider all surveys that have properly reported null detections and detection limits (e.g., Sartoretti et al. 1998; Massarotti et al. 2005; Tanner et al. 2007; Lafrenière et al. 2008a; Metchev & Hillenbrand 2009; Chauvin et al. 2010). Chauvin et al. (2010) reported one detection (AB Pic) from 30–40 young solar-type targets surveyed (depending on the definitions of "young" and "solar type"). Indeed, the full sample of past null detections is larger than our observed sample, suggesting that the true frequency could be lower by up to a factor of $\gtrsim$2, and that our survey had good fortune to discover two new companions. Alternatively, including the companions to CT Cha and possibly GQ Lup (likely more massive than 20 $M_{\rm J}$) may increase the true frequency of wide ULMCs, if only the details of the survey samples in which these companions were discovered were known. A large census of the literature is beyond the scope of a discovery paper, and the results of this analysis will be reported in a companion paper (A. L. Kraus et al. 2011, in preparation).

**Table 4**
Detection Limits for Additional Companions

| Name | $K_{\rm lim}$ (mag) at $\rho$ = (mas) | | | | | | | $M_{\rm lim}$ ($M_{\rm Jup}$) at $\rho$ = (AU) | | | | | | | $\rho_{100\%}$ |
|---|---|---|---|---|---|---|---|---|---|---|---|---|---|---|---|
| | 300 | 400 | 500 | 750 | 1000 | 1500 | ⩾2000 | 45 | 60 | 75 | 110 | 150 | 225 | ⩾300 | ($''$) |
| GSC 06205−00954 | 12.9 | 13.4 | 13.4 | 14.1 | 15.0 | 16.4 | 17.8 | 42 | 28 | 28 | 21 | 14 | 6.9 | 4.5 | 10.4 |
| GSC 06208−00834 | 12.6 | 13.5 | 13.6 | 14.0 | 14.8 | 16.4 | 17.5 | 57 | 27 | 26 | 22 | 16 | 6.8 | 4.7 | 10.7 |
| GSC 06209−01501 | 12.3 | 13.3 | 13.1 | 13.7 | 14.8 | 16.1 | 17.7 | 74 | 30 | 33 | 25 | 16 | 7.6 | 4.5 | 10.4 |
| GSC 06213−00194 | 12.1 | 12.7 | 13.3 | 13.6 | 14.0 | 15.7 | 17.1 | 78 | 52 | 30 | 26 | 22 | 11 | 5.4 | 10.2 |
| GSC 06213−01358 | 12.9 | 13.6 | 13.8 | 14.2 | 15.2 | 16.5 | 17.9 | 39 | 26 | 23 | 20 | 14 | 6.5 | 4.4 | 10.4 |
| GSC 06214−00210 | 12.5 | 13.3 | 13.8 | 14.6 | 14.8 | 16.0 | 17.4 | 62 | 29 | 24 | 17 | 16 | 8.4 | 4.8 | 9.4 |
| GSC 06214−02384 | 12.3 | 12.9 | 13.5 | 13.9 | 14.4 | 15.8 | 17.5 | 76 | 41 | 27 | 23 | 18 | 9.9 | 4.8 | 10.2 |
| GSC 06764−01305 | 12.4 | 13.1 | 13.6 | 14.1 | 14.8 | 16.2 | 16.9 | 71 | 33 | 27 | 21 | 16 | 7.4 | 5.7 | 11.1 |
| GSC 06793−00797 | 11.7 | 12.9 | 13.2 | 13.8 | 14.4 | 16.0 | 17.3 | 97 | 42 | 31 | 24 | 19 | 8.3 | 5.0 | 10.2 |
| GSC 06793−00994 | 12.1 | 12.8 | 13.4 | 13.5 | 14.1 | 15.7 | 17.2 | 78 | 43 | 29 | 28 | 21 | 10 | 5.2 | 10.2 |
| GSC 06794−00156 | 9.8 | 10.7 | 11.4 | 12.1 | 12.9 | 14.6 | 17.2 | 413 | 212 | 130 | 78 | 41 | 17 | 5.1 | 10.2 |
| GSC 06794−00480 | 12.0 | 12.7 | 13.1 | 13.8 | 13.9 | 16.0 | 17.0 | 81 | 53 | 33 | 24 | 23 | 8 | 5.5 | 10.2 |
| GSC 06794−00537 | 11.9 | 12.7 | 13.1 | 13.6 | 14.0 | 15.7 | 17.7 | 89 | 54 | 34 | 26 | 22 | 10 | 4.6 | 10.2 |
| RXJ1550.0−2312 | 13.7 | 14.4 | 15.1 | 16.8 | 17.4 | 17.2 | 17.1 | 25 | 19 | 14 | 5.8 | 4.9 | 5.1 | 5.4 | 2.1 |
| RXJ1550.9−2534 | 11.4 | 12.8 | 13.8 | 15.6 | 16.8 | 17.1 | 17.3 | 129 | 44 | 24 | 11 | 5.9 | 5.4 | 4.9 | 1.3 |
| RXJ1551.1−2402 | 14.3 | 15.5 | 15.8 | 17.0 | 17.1 | 17.1 | 17.2 | 19 | 12 | 10 | 5.5 | 5.3 | 5.3 | 5.2 | 1.5 |
| RXJ1557.8−2305 | 13.7 | 15.0 | 15.5 | 16.9 | 17.3 | 17.2 | 17.1 | 25 | 15 | 12 | 5.7 | 4.9 | 5.1 | 5.4 | 3.7 |
| RXJ1558.1−2405 | 11.4 | 12.5 | 13.2 | 14.1 | 14.6 | 16.1 | 17.0 | 126 | 64 | 32 | 21 | 17 | 7.7 | 5.6 | 8.9 |
| RXJ1558.2−2328 | 11.4 | 12.1 | 12.7 | 13.3 | 13.9 | 15.4 | 17.1 | 128 | 78 | 54 | 29 | 23 | 12 | 5.2 | 10.2 |
| RXJ1600.7−2127 | 12.5 | 13.6 | 14.1 | 14.2 | 15.0 | 16.3 | 17.6 | 61 | 26 | 21 | 20 | 15 | 7.1 | 4.6 | 10.6 |
| RXJ1601.1−2113 | 12.7 | 13.4 | 13.5 | 13.7 | 14.8 | 16.5 | 17.4 | 56 | 28 | 27 | 25 | 16 | 6.6 | 4.8 | 9.6 |
| RXJ1601.9−2008 | 11.7 | 12.2 | 12.3 | 12.9 | 13.5 | 15.6 | 17.6 | 101 | 76 | 72 | 39 | 28 | 11 | 4.6 | 11 |
| RXJ1602.0−2221 | 13.1 | 14.4 | 15.1 | 16.8 | 16.9 | 17.0 | 17.1 | 35 | 19 | 14 | 5.8 | 5.7 | 5.5 | 5.3 | 3.7 |
| RXJ1602.8−2401A | 11.1 | 11.8 | 12.4 | 14.1 | 15.0 | 16.0 | 17.0 | 156 | 95 | 71 | 20 | 15 | 8.4 | 5.6 | 3.6 |
| RXJ1602.8−2401B | 10.1 | 10.6 | 11.3 | 12.4 | 13.3 | 14.7 | 15.1 | 332 | 226 | 131 | 67 | 30 | 16 | 14.0 | 10.2 |
| RXJ1603.6−2245 | 11.9 | 12.7 | 13.4 | 13.8 | 14.4 | 15.8 | 17.4 | 89 | 54 | 28 | 24 | 19 | 9.3 | 4.8 | 10.2 |
| RXJ1603.9−2031A | 11.9 | 12.7 | 13.4 | 13.6 | 14.5 | 16.0 | 17.6 | 88 | 54 | 29 | 27 | 18 | 8.4 | 4.6 | 10.1 |
| RXJ1604.3−2130 | 11.9 | 12.3 | 13.0 | 13.7 | 14.3 | 15.9 | 17.1 | 83 | 73 | 37 | 25 | 19 | 8.7 | 5.2 | 8.9 |
| RXJ1606.2−2036 | 10.4 | 11.1 | 11.7 | 12.8 | 13.5 | 15.1 | 15.4 | 271 | 164 | 96 | 45 | 27 | 14 | 12.0 | 11.1 |
| RXJ1607.0−2036 | 9.1 | 12.4 | 13.3 | 13.9 | 14.5 | 15.6 | 17.9 | 648 | 69 | 30 | 23 | 18 | 11 | 4.3 | 8.7 |
| ScoPMS015 | 11.3 | 13.4 | 13.8 | 14.1 | 15.1 | 16.9 | 17.9 | 140 | 28 | 24 | 20 | 14 | 5.7 | 4.3 | 10.4 |
| ScoPMS017 | 13.9 | 14.7 | 15.0 | 16.9 | 17.6 | 17.4 | 17.2 | 23 | 17 | 15 | 5.7 | 4.6 | 4.9 | 5.2 | 1.5 |
| ScoPMS019 | 11.3 | 12.1 | 12.5 | 13.5 | 13.9 | 15.5 | 16.6 | 133 | 79 | 65 | 27 | 23 | 11 | 6.2 | 8.8 |
| ScoPMS022 | 14.3 | 15.5 | 15.5 | 17.4 | 17.4 | 17.3 | 17.3 | 19 | 12 | 12 | 4.9 | 4.9 | 4.9 | 5.0 | 1.4 |
| ScoPMS027 | 11.8 | 12.6 | 12.7 | 12.9 | 13.5 | 15.3 | 16.4 | 89 | 57 | 49 | 42 | 28 | 13 | 6.9 | 3.0 |
| ScoPMS028 | 13.1 | 15.0 | 15.9 | 17.1 | 17.2 | 17.0 | 16.9 | 34 | 15 | 9.3 | 5.3 | 5.1 | 5.4 | 5.7 | 3.7 |
| ScoPMS044 | 11.8 | 12.3 | 12.7 | 13.0 | 13.4 | 15.5 | 17.7 | 91 | 72 | 53 | 36 | 28 | 12 | 4.5 | 10.3 |
| ScoPMS045 | 12.8 | 13.4 | 13.8 | 14.2 | 14.6 | 15.8 | 18.0 | 48 | 28 | 24 | 20 | 17 | 9.6 | 4.2 | 10.7 |
| USco-160341.8−200557 | 14.0 | 15.4 | 15.7 | 17.3 | 17.4 | 17.4 | 17.3 | 22 | 12 | 10 | 5 | 4.8 | 4.9 | 5.0 | 2.2 |
| USco-160643.8−190805 | 10.1 | 10.8 | 11.6 | 13.2 | 13.8 | 15.6 | 15.8 | 336 | 203 | 110 | 30 | 24 | 11 | 9.4 | 8.5 |
| USco-160707.7−192715 | 14.6 | 16.1 | 16.6 | 17.9 | 17.9 | 17.7 | 17.6 | 17 | 7.6 | 6.2 | 4.4 | 4.3 | 4.5 | 4.7 | 1.5 |
| USco-160801.4−202741 | 11.1 | 11.9 | 12.5 | 13.7 | 14.1 | 15.8 | 16.1 | 158 | 86 | 64 | 25 | 20 | 10 | 7.8 | 8.5 |
| USco-160823.2−193001 | 14.4 | 15.5 | 15.7 | 17.3 | 17.4 | 17.3 | 17.3 | 18 | 11 | 11 | 5 | 4.9 | 5.0 | 5.0 | 3.7 |
| USco-160825.1−201224 | 14.3 | 15.8 | 16.3 | 17.3 | 17.5 | 17.5 | 17.5 | 19 | 10 | 7 | 4.9 | 4.8 | 4.8 | 4.8 | 1.5 |
| USco-160900.7−190852 | 10.8 | 11.5 | 12.2 | 13.6 | 14.1 | 15.6 | 16.0 | 196 | 115 | 76 | 26 | 21 | 11 | 8.3 | 6.0 |
| USco-160916.8−183522 | 14.3 | 15.8 | 16.0 | 17.4 | 17.7 | 17.6 | 17.4 | 19 | 9.6 | 8.1 | 4.9 | 4.5 | 4.7 | 4.9 | 2.1 |
| USco-160954.4−190654 | 14.5 | 15.5 | 16.0 | 17.4 | 17.4 | 17.5 | 17.5 | 18 | 12 | 8.4 | 4.9 | 4.9 | 4.8 | 4.7 | 2.2 |
| USco-161031.9−191305 | 10.8 | 11.5 | 12.2 | 13.3 | 13.9 | 15.5 | 16.1 | 200 | 114 | 77 | 29 | 23 | 12 | 7.7 | 8.5 |
| USco-161347.5−183459 | 13.4 | 13.5 | 13.5 | 13.4 | 13.3 | 13.2 | 13.1 | 28 | 27 | 27 | 29 | 29 | 31 | 34 | 2.1 |

**Notes.** Detection limits are $5\sigma$ for all columns except for the ⩾2000 mas and ⩾300 AU columns, where they are $10\sigma$. The 5 Myr isochrones of the DUSTY models were used to compute $K$ magnitudes. $\rho_{100\%}$ refers to the maximum separation where our survey is 100% complete for additional companions.

## 5. DISCUSSION: IMPLICATIONS FOR FORMATION MECHANISM

The population of directly imaged wide ($\gtrsim$40 AU) ULMCs poses a significant challenge to planet formation models. Existing models of solar system scale planet formation (i.e., via core accretion or gravitational instability in a Class II disk; Pollack et al. 1996) have not been successful at forming planets at the orbital radii they are observed here ($\gtrsim$200 AU). It is also difficult to form wide ULMCs like a binary (i.e., via fragmentation of the free-falling protostellar core or fragmentation in the massive protostellar disk) without subsequently accreting sufficient mass to become a stellar or brown dwarf companion. However, one of these mechanisms must occur. Complicating this picture is the possibility, and indeed likelihood, of multiple planet scattering in some formation scenarios. Therefore, we cannot answer the question of formation mechanism without examining the population of ULMCs in separation and mass space alongside more well-studied classes of companions.

The core accretion mechanism for planetary formation only operates close to the host star ($\sim$5 AU), where protoplanetary disk densities are high enough to enable dust and ice to coagulate into protoplanets. Therefore, a wide ULMC could only originate from core accretion if it came from a scattering event. In any scattering event, low-mass companions are preferentially scattered outward, so a core accretion and scattering origin for

wide ULMCs would require an even greater population of close, higher-mass objects. As brown dwarfs are well known to be rare less than ∼5 AU from their host stars (the "brown dwarf desert"; Marcy & Butler 2000), this scenario is very unlikely.

Another plausible formation scenario for wide ULMCs appears to be formation like stars from the fragmentation of protostellar clouds and massive circumstellar disks (e.g., Kratter et al. 2010). In existing models, it is difficult to form ULMCs because fragments subsequently accrete mass, and the only fragments that remain near the opacity limit for fragmentation are those that are ejected (Bate et al. 2002). In an extreme case, the fragmentation of each core might be expected to be independent and companions would be expected to follow an initial mass function (i.e., random pairing). This is now well known to be incorrect, with an approximately linearly flat distribution of companion masses for solar-type primaries and $\sim 10^2$ AU separations (Kraus et al. 2008; Raghavan et al. 2010; A. L. Kraus et al. 2011, in preparation). As young solar-type stars have stellar companion fractions in the range 12%–22% (Brandner et al. 1996; K08; A. L. Kraus et al. 2011, in preparation) per decade of separation, this would mean that 0.2%–0.3% of solar-type stars should have ∼50–500 AU, $q = 0.006$–$0.02$ companions (i.e., 6–20 $M_J$ for solar-type stars. We see a clear surplus to this model, strongly suggesting that wide ULMCs follow a different formation path to stars.

If wide ULMCs were to form via fragmentation of a circumstellar disk when the primary is at the Class II stage (disk masses 0.001–0.1 $M_\odot$; e.g., Boss 2001) it would be much easier to form wide companions than with core accretion. Although most observed disks have masses of $\sim 5$ $M_J$, a few disks around solar-type stars (e.g., DL Tau) have large enough linear dimensions and mass (up to ∼1000 AU and 0.1 $M_\odot$; Andrews & Williams 2005, 2007) to fragment into observed ULMCs. Relatively little work has been done examining in detail how these large disks might fragment, with the bulk of disk-fragmentation literature discussing the possible formation of solar system scale planets via fragmentation. Where models of large disks have been computed (e.g., Meru & Bate 2010), it is clear that it is easier for them to become Toomre unstable and fragment than ∼20 AU disks. The remaining questions to be answered about this fragmentation include how many fragments are expected, and if the fragments can accrete enough of the disk mass to become objects like GSC 06214−00210b and 1RXS J160929.1−210524 b.

The question of where each formation mechanism operates is certainly not answered yet, but could be in the next few years. Radial velocity techniques will provide real constraints on the ∼5–10 AU giant planet frequency as their time baselines increase, while direct imaging surveys will finish probing the wide ULMC frequency around young stars. Finally, high-angular resolution techniques such as aperture-masking and high-efficiency coronagraphy will fill much of the yet unprobed ∼5–30 AU regime of orbital separations which likely forms the boundary between the dominance of core accretion and fragmentation processes.

M.I. acknowledges support from the Australian Research Council through an Australian Postdoctoral Fellowship. We thank undergraduate students Alison Hammond and Matthew Hill from the University of Sydney, who made a first-pass astrometric analysis of the data. We also thank Mike Liu, Brendan Bowler, and the anonymous referee for helpful detailed comments on the manuscript. A.L.K. was supported by a SIM Science Study and by NASA through Hubble Fellowship grant 51257.01 awarded by the Space Telescope Science Institute, which is operated by the Association of Universities for Research in Astronomy, Inc., for NASA, under contract NAS 5-26555. This work is based in part on data obtained as part of the UKIRT Infrared Deep Sky Survey. Some of these observations were obtained at the Hale Telescope at Palomar Observatory, as part of a collaborative agreement between the California Institute of Technology, JPL, and Cornell University. Some of the data presented herein were obtained at the W.M. Keck Observatory, which is operated as a scientific partnership among the California Institute of Technology, the University of California, and the National Aeronautics and Space Administration. The Observatory was made possible by the generous financial support of the W.M. Keck Foundation. The authors wish to recognize and acknowledge the very significant cultural role and reverence that the summit of Mauna Kea has always had within the indigenous Hawaiian community. We are most fortunate to have the opportunity to conduct observations from this mountain.

## REFERENCES

Allen, P. R. 2007, ApJ, 668, 492
Allers, K. N., Liu, M. C., Dupuy, T. J., & Cushing, M. C. 2010, ApJ, 715, 561
Anderson, D. R., et al. 2011, ApJL, in press (arXiv:1010.3006)
Andrews, S. M., & Williams, J. P. 2005, ApJ, 631, 1134
Andrews, S. M., & Williams, J. P. 2007, ApJ, 659, 705
Baraffe, I., Chabrier, G., Allard, F., & Hauschildt, P. H. 1998, A&A, 337, 403
Baraffe, I., Chabrier, G., Barman, T. S., Allard, F., & Hauschildt, P. H. 2003, A&A, 402, 701
Bate, M. R. 2005, MNRAS, 363, 363
Bate, M. R., Bonnell, I. A., & Bromm, V. 2002, MNRAS, 332, L65
Béjar, V. J. S., Zapatero Osorio, M. R., Pérez-Garrido, A., Álvarez, C., Martín, E. L., Rebolo, R., Villó-Pérez, I., & Díaz-Sánchez, A. 2008, ApJ, 673, L185
Bertin, E., & Arnouts, S. 1996, A&AS, 117, 393
Boley, A. C. 2009, ApJ, 695, L53
Boss, A. P. 2001, ApJ, 563, 367
Bouchy, F., Deleuil, M., Guillot, T., Aigrain, S., Carone, L., & Cochran, W. D. 2011, A&A, 525, A68
Brandner, W., Alcala, J. M., Kunkel, M., Moneti, A., & Zinnecker, H. 1996, A&A, 307, 121
Cameron, B. P. 2008, PhD thesis, California Institute of Technology
Cameron, P. B., Britton, M. C., & Kulkarni, S. R. 2009, AJ, 137, 83
Chabrier, G., Baraffe, I., Allard, F., & Hauschildt, P. 2000, ApJ, 542, 464
Chauvin, G., Lagrange, A., Dumas, C., Zuckerman, B., Mouillet, D., Song, I., Beuzit, J., & Lowrance, P. 2004, A&A, 425, L29
Chauvin, G., et al. 2010, A&A, 509, A52
Currie, T., Lada, C. J., Plavchan, P., Robitaille, T. P., Irwin, J., & Kenyon, S. J. 2009, ApJ, 698, 1
Deleuil, M., et al. 2008, A&A, 491, 889
de Zeeuw, P. T., Hoogerwerf, R., de Bruijne, J. H. J., Brown, A. G. A., & Blaauw, A. 1999, AJ, 117, 354
Fluks, M. A., Plez, B., The, P. S., de Winter, D., Westerlund, B. E., & Steenman, H. C. 1994, A&AS, 105, 311
Ghez, A. M., Neugebauer, G., & Matthews, K. 1993, AJ, 106, 2005
Ghez, A. M., et al. 2008, ApJ, 689, 1044
Golimowski, D. A., et al. 2004, AJ, 127, 3516
Grether, D., & Lineweaver, C. H. 2006, ApJ, 640, 1051
Haisch, K. E., Jr., Lada, E. A., & Lada, C. J. 2001, ApJ, 553, L153
Hernández, J., et al. 2007, ApJ, 662, 1067
Hillenbrand, L. A., & White, R. J. 2004, ApJ, 604, 741
Hoyle, F. 1953, ApJ, 118, 513
Kalas, P., et al. 2008, Science, 322, 1345
Kratter, K. M., Murray-Clay, R. A., & Youdin, A. N. 2010, ApJ, 710, 1375
Kraus, A. L. 2009, PhD thesis, California Institute of Technology
Kraus, A. L., & Hillenbrand, L. A. 2007, AJ, 134, 2340
Kraus, A. L., & Hillenbrand, L. A. 2008, ApJ, 686, L111
Kraus, A. L., & Hillenbrand, L. A. 2009, ApJ, 703, 1511
Kraus, A. L., Ireland, M. J., Martinache, F., & Lloyd, J. P. 2008, ApJ, 679, 762 (K08)
Kunkel, M. 1999, PhD thesis, Univ. Wurzburg

Lafrenière, D., Jayawardhana, R., Brandeker, A., Ahmic, M., & van Kerkwijk, M. H. 2008a, ApJ, 683, 844
Lafrenière, D., Jayawardhana, R., & van Kerkwijk, M. H. 2008b, ApJ, 689, L153
Lafrenière, D., Jayawardhana, R., & van Kerkwijk, M. H. 2010, ApJ, 719, 497
Lafrenière, D., et al. 2007, ApJ, 670, 1367
Lawrence, A., et al. 2007, MNRAS, 379, 1599
Leggett, S. K. 1992, ApJS, 82, 351
Leggett, S. K., et al. 2002, ApJ, 564, 452
Lodieu, N., Hambly, N. C., Jameson, R. F., Hodgkin, S. T., Carraro, G., & Kendall, T. R. 2007, MNRAS, 374, 372
Low, C., & Lynden-Bell, D. 1976, MNRAS, 176, 367
Mamajek, E. E. 2005, ApJ, 634, 1385
Marcy, G. W., & Butler, R. P. 2000, PASP, 112, 137
Marois, C., Macintosh, B., Barman, T., Zuckerman, B., Song, I., Patience, J., Lafrenière, D., & Doyon, R. 2008, Science, 322, 1348
Masciadri, E., Mundt, R., Henning, T., Alvarez, C., & Barrado y Navascués, D. 2005, ApJ, 625, 1004
Massarotti, A., Latham, D. W., Torres, G., Brown, R. A., & Oppenheimer, B. D. 2005, AJ, 129, 2294
Meru, F., & Bate, M. R. 2010, MNRAS, 406, 2279
Metchev, S. A., & Hillenbrand, L. A. 2009, ApJS, 181, 62
Monet, D. G., et al. 2003, AJ, 125, 984
Pollack, J. B., Hubickyj, O., Bodenheimer, P., Lissauer, J. J., Podolak, M., & Greenzweig, Y. 1996, Icarus, 124, 62
Preibisch, T., Guenther, E., Zinnecker, H., Sterzik, M., Frink, S., & Roeser, S. 1998, A&A, 333, 619
Raghavan, D., et al. 2010, ApJS, 190, 1
Sartoretti, P., Brown, R. A., Latham, D. W., & Torres, G. 1998, A&A, 334, 592
Schlegel, D. J., Finkbeiner, D. P., & Davis, M. 1998, ApJ, 500, 525
Scholz, A., Jayawardhana, R., Wood, K., Meeus, G., Stelzer, B., Walker, C., & O'Sullivan, M. 2007, ApJ, 660, 1517
Simon, M., et al. 1995, ApJ, 443, 625
Stamatellos, D., & Whitworth, A. P. 2009, MNRAS, 392, 413
Stetson, P. B. 1987, PASP, 99, 191
Tanner, A., et al. 2007, PASP, 119, 747
Teixeira, R., Ducourant, C., Chauvin, G., Krone-Martins, A., Song, I., & Zuckerman, B. 2008, A&A, 489, 825
Troy, M., et al. 2000, Proc. SPIE, 4007, 31
van Leeuwen, F. 2007, A&A, 474, 653
Zacharias, N., et al. 2010, AJ, 139, 2184